

# The Characteristic of the Large-amplitude Pulsation in a Model Yellow Supergiant Star

著者	TAKEUTI Mine, NAKATA Michinori, AIKAWA Toshiki
journal or publication title	The science reports of the Tohoku University. Ser. 8, Physics and astronomy
volume	5
number	3
page range	180-187
year	1985-01-25
URL	<a href="http://hdl.handle.net/10097/25550">http://hdl.handle.net/10097/25550</a>

The Characteristic of the Large-amplitude Pulsation  
in a Model Yellow Supergiant Star

Mine TAKEUTI, Michinori NAKATA and Toshiki AIKAWA\*  
Astronomical Institute, Faculty of Science,  
Tôhoku University, Sendai 980

\*Department of Physics and Astronomy, University of  
Nebraska-Lincoln, Lincoln, NE 68588-0111, U.S.A.

(Received December 14, 1984)

The large-amplitude pulsation of a model yellow supergiant star is investigated by using a hydrodynamic code. The parameters of the model were  $M = 1 M_{\odot}$ ,  $L = 3200 L_{\odot}$  and  $T_{\text{eff}} = 5300$  K. The recurrence of the generation of strong shock wave is obtained in every several pulsation periods. The abrupt decrease of the pulsation period has found after the formation of extended atmospheres above the photosphere. The outer boundary conditions for the linear non-adiabatic approximation derived by Castor fail to reproduce this period.

Keywords: Stellar pulsation, Supergiant stars, Extended atmospheres.

## §1. Introduction

While many authors have performed hydrodynamic simulation for various pulsating stars, we have had only less systematic views on the pulsation of models whose surface gravity is much lesser than that of classical cepheids. First Christy<sup>1)</sup> tried the hydrodynamical simulation on the population II cepheids and then Keeley<sup>2)</sup> studied long-period red variable stars. The difficulty in the hydrodynamic study of low-surface-gravity models are mainly concerning with the increase of amplitudes and the generation of strong shock wave. So the simulation requires much more computational time than the RR Lyrae stars and classical cepheids. The models of less massive supergiant stars were studied by Trimble<sup>3)</sup> and very violent pulsation was found. Wood<sup>4)</sup> and King<sup>5)</sup> have obtained the similar results. Tuchman, Sach and Barkat<sup>6)</sup> performed the simulation of red giant models following Keeley. Fadeyev and Tutukov<sup>7)</sup> and Fadeyev<sup>8)</sup> calculated the hydrodynamical models of yellow supergiant stars. Recently Fadeyev<sup>9)</sup> tried in running his hydrodynamic code HYDRA for studying a very low-surface-gravity models and found an almost steady mass-loss.

In the present paper, we described the properties of the hydrodynamic simulation for a model yellow supergiant star which has the similar parameters to the model investigated by Fadeyev and Tutukov<sup>7)</sup>. The results are essentially the same as those of Fadeyev and Tutukov, but the decrease of the pulsation

period has found after the generation of very strong shock wave. We discussed the outer boundary conditions of stellar pulsation briefly.

## §2. Hydrodynamic Models

The DYN-code, originally constructed by Castor et al.<sup>10)</sup> for the hydrodynamic simulation of classical cepheids, was preferred, because the rezoning procedure working in the DYN makes oscillation very smooth. The results obtained by our DYN-code were described previously<sup>11)</sup>. For the present study, the code has been partly modified to investigate more precisely the motion of extended atmospheres. The procedure to construct outer atmospheres in the static model was changed to the iterative one to set the stellar radius  $R$  to be equal to the radius  $R_{2/3}$ , the radius at  $\tau = 2/3$ , i.e. the radius of outermost interface,  $R_{N+1}$ , is determined by an iterative procedure as  $R_{2/3}$  fits to the given stellar radius  $R$  in the improved code. Then the relation

$$L_{2/3} = 4 \pi R_{2/3}^2 \sigma T_{2/3}^4, \quad (1)$$

where  $L_{2/3}$  and  $T_{2/3}$  were the luminosity and the temperature at  $\tau = 2/3$ , holds exactly at the initial stage. This improvement is not efficient for calculating model cepheids, but it is necessary for less-massive models like as the models studied in the present paper.

The linear growth rate of the fundamental mode depends very sensitively on the effective temperature for the models studied here of which the parameters were  $M = 1 M_{\odot}$  and  $L = 3200 L_{\odot}$ . The growth rate of yellow supergiant stars are studied in detail by Aikawa<sup>12)</sup>. In the present study, the model of  $T_{\text{eff}} = 5500$  K were weakly unstable<sup>13)</sup> besides that of  $T_{\text{eff}} = 5000$  K is strongly unstable. So the effective temperature  $T_{\text{eff}} = 5300$  K was chosen for the model intensively studied. In the latter the pulsation still grows up, although the growth rate is nearly a half of that for the model of  $T_{\text{eff}} = 5000$  K. It became easier to investigate the pulsation over many cycles when the growth rate is small. The radius of the innermost interface  $R_1$  was set as  $0.05 R_{2/3}$  and the optical depth of the outermost interface was  $0.0005$ . The ratio of masses of successive shells was  $1.30$  for expressing the extended envelopes more smoothly. So the model consisted of  $91$  zones and  $16$  of them were found above the layer of  $\tau = 2/3$  at the initial model. The total mass of model envelope was  $3.60 \times 10^{-3} M_{\odot}$ . The opacity was calculated by Stellingwerf's formula for the population I mixture, the King IVa mixture ( $X = 0.70$ ,  $Y = 0.28$ ,  $Z = 0.02$ ), as the same as Takeuti's note<sup>13)</sup>. The constant  $C_0$  in the expression on the artificial viscosity was fixed at  $4.0$  for smoothing the oscillation.

The initial velocity distribution was given by the following formula.

$$U_i/U_0 = 1.63 (R_i/R_{91})^{6.3} - 0.63 (R_i/R_{91})^{16.3}, \quad (2)$$

where the  $91$ st interface is the outermost one in the model and  $R_i$  and  $R_{91}$

indicate the radii of the  $i$ -th and 91st one, respectively. This formula was chosen also for smoothing the oscillation, even the effect was not so remarkable. In the present calculation, the velocity of the outermost interface  $U_{91}$  was chosen as  $-10 \text{ km sec}^{-1}$ . In the course of calculation, we removed the interface where the velocity exceeded the local escape velocity out of calculation.

### §3. Results

Results are shown in Figs. 1-4. The light curve  $L_{2/3}$  and the photospheric radial-velocity curve  $U_{2/3}$ , demonstrated in Figs. 1 and 2 respectively, do not

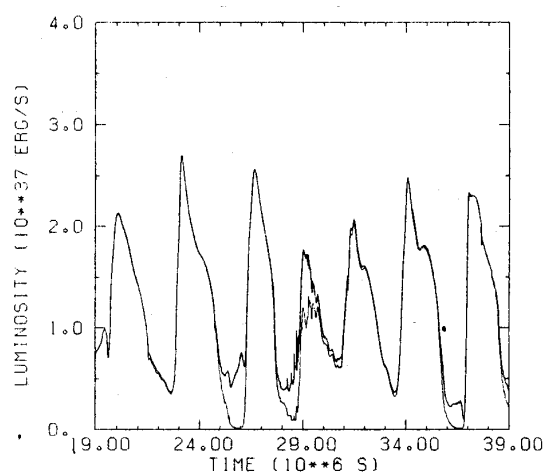


Fig. 1. Light curves. Thin curve indicates  $L_{2/3}$  and thick one is  $L_{91}$ , the luminosity at the outermost interface.

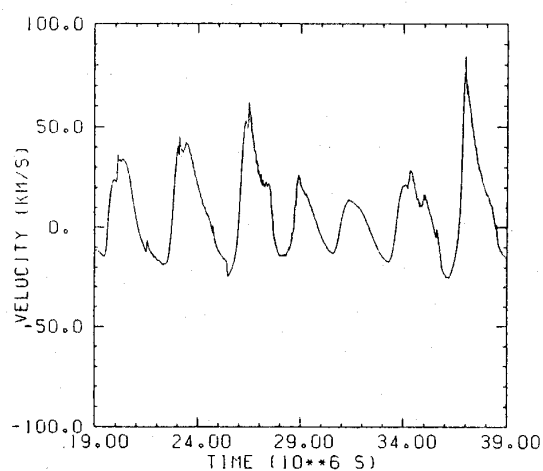


Fig. 2. Photospheric radial-velocity curve.

seem so singular, look like a regular periodic pulsation with variable amplitude. The period is  $3 \times 10^6$  sec or less while the period calculated in the linear adiabatic approximation is  $4.02 \times 10^6$  sec (46.5 days) for the fundamental mode and  $1.56 \times 10^6$  sec (18.1 days) for the first overtone. The problem of periods will be discussed later. In Fig. 1 the thick line indicates the emergent flux from the outermost interface  $L_{91}$ . The thin line is the photospheric light curve. The discrepancy found in the violent phases between them expresses the inadequacy of the diffusion approximation.

In Fig. 3, the time-variation of several Lagrangian radii are illustrated. They show quite different appearance with those of small-amplitude pulsation. The uppermost thick line shows  $R_{91}$  outside of which only  $5 \times 10^{-5}$  % of the total stellar mass is included, and the undermost thick line shows the motion of the interface inside of which 99.96 % of the total mass is included.  $R_{91}$  reaches about four times high compared with the radius of static model with the enhancement of oscillation and then  $U_{91}$  exceeds the local escape velocity. The thin line illustrates the time-variation of the photospheric radius. We

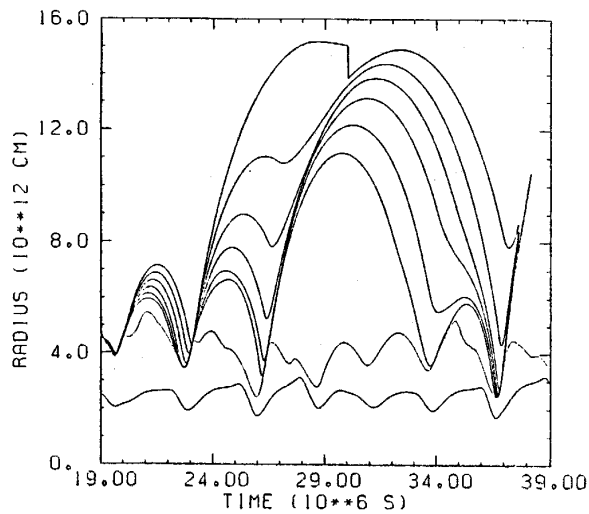


Fig. 3. Time variation of radii of Lagrangian shells  $R_1$ . Thick lines indicate the radius of 91st interface and the Lagrangian trajectories in the atmosphere, respectively. Thin line expresses the photospheric radius  $R_{2/3}$ . The discontinuity of  $R_{91}$  appeared at  $30 \times 10^6$  sec indicates the sudden drop of the shell caused by the artificial suppression of the kinetic energy of the outermost shell at the passage of very strong shock wave.

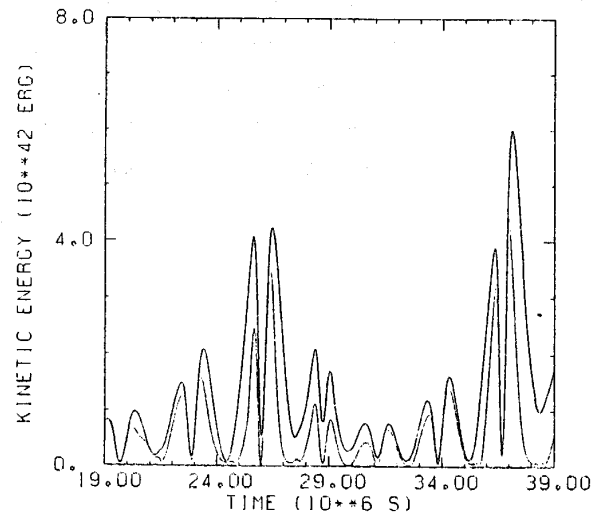


Fig. 4. Time variation of the kinetic energy. Thick line indicates the total kinetic energy and thin line expresses the kinetic energy included in sub-photospheric layers.

can see the photosphere follows the movement of deep envelopes in comparatively high fidelity.

The total kinetic energy  $K$ , illustrated by the thick line in Fig. 4, shows a couple of peaks every period. They correspond to the infalling and rising-up phases respectively. The thin line shows the sum of kinetic energy of the layers under the photosphere. So the difference between the thick and thin lines in Fig. 4 shows the kinetic energy including optically thin layers. While the amplitude of oscillation grows up, the kinetic energy of optically thin layers becomes greater. This corresponds to the formation of extended atmospheres above the photosphere. It is worthy of noting that the maximum kinetic energy  $K_{\max}$  increases with the time first, and then the strong shock wave is generated by expense of the pulsation energy. Because of the transition of the energy from the sub-photospheric shells to the outer atmospheres, the pulsation reincreases by the unstable nature of the envelopes and the strong shock wave again runs out after the pulsation has grown up. We can see this cyclic behaviour of pulsation also in the figure of Fadeyev and Tutukov's paper<sup>7)</sup>.

§4. Discussions on the Pulsation Periods

The periods found in the present simulation are tabulated in Table 1.

Table 1. Periods of successive cycles of model.

time (in $10^6$ sec)	period (in $10^6$ sec)
4.58	3.08
7.64	3.06
10.76	3.11
13.93	3.18
17.13	3.20
20.33	3.20
23.40	3.07
26.47	3.07
29.05	2.58
31.64	2.59
34.31	2.68
37.14	2.83
39.86	2.72
42.56	2.69
45.03	2.48

Linear adiabatic period: 4.02  
 Linear non-adiabatic period (Castor's conditions): 3.11  
 Linear non-adiabatic period (Takeuti's conditions): 2.59

The period tabulated is the time interval between the time of the kinetic energy maximum indicated at the left and the time of the last but one preceding kinetic energy maximum. At the bottom of the table, the linear adiabatic period, the linear non-adiabatic period calculated by using Castor's boundary conditions<sup>14)</sup> and that by using Takeuti's boundary conditions<sup>15)</sup> are described. For model classical cepheids, the effect of outer boundary conditions used here on the linear non-adiabatic period is negligibly small, but the present case the period determined by using Takeuti's ones is 20 % shorter than that by using Castor's ones. This is typical for the models which have extended atmospheres.

The periods tabulated in Table 1 show a remarkable feature that the period is very similar to the period derived by using Castor's boundary conditions at the earlier stage of the simulation. The period decreases abruptly when the strong shock wave passes through the atmosphere and the extended atmosphere is formed. And then the period becomes more similar to that calculated by using Takeuti's conditions. We shall discuss here the problem of pulsation periods. The outer boundary conditions for linear pulsation were a problem in the course of the investigation of classical

cepheids. Baker and Kippenhahn<sup>16)</sup> concluded that the difference in outer boundary conditions is not so serious for studying classical cepheids and we have usually use Castor's one. The pulsation function of the system of linear equations are certainly different between the adiabatic case and the non-adiabatic case. And the outer boundary conditions of the DYN-code are the same ones as Castor's linear boundary conditions at the outermost surface. So the agreement in periods between non-linear case and linear case based on Castor's condition is reasonable. Takeuti's conditions are other extreme case to Castor's one, because it is diffined as the relationship at the photospheric layer ( $\tau = 2/3$ ). This is based on the assumption that atmospheres stay in the radiative equilibrium through the pulsation and the atmospheric layers above the photosphere follow smoothly the motions of photosphere. This picture seems to be suitable to the oscillation of extended atmospheres. Takeuti's conditions ignore detailed hydrodynamical interaction of the second order in outer atmospheres, however. We can only point out here that the latter conditions yield shorter periods.

The density distribution with the radii relative to the instantaneous photospheric radius is illustrated in Fig. 5a and Fig. 5b. It is clear that

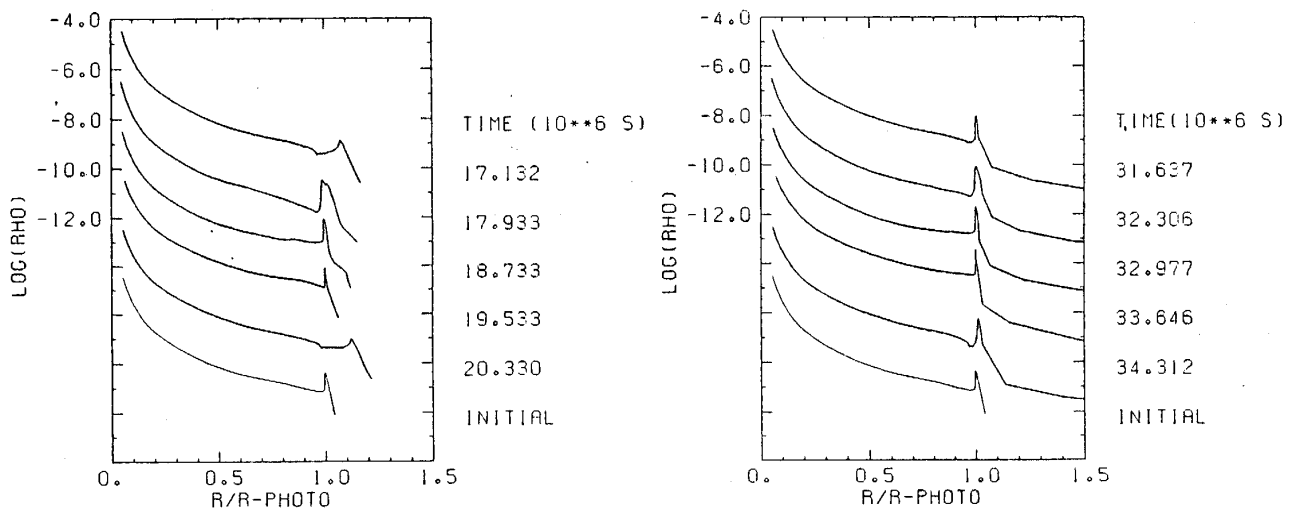


Fig. 5a. Density distribution with the relative radius at phases before the generation of strong shock. Abscissa is the radius relative to the instantaneous radius at  $\tau = 2/3$ . Ordinate is the logarithm of density. The scase is shifted for each curve with the interval of 2.0. Figures written at the right hand side are the time from the start of simulation. First and fifth curves express the distribution at the kinetic energy maximum phase in expansion. The undermost curve indicates the initial density distribution, i.e. the density distribution of the static model.

Fig. 5b. The same as Fig. 5a for phases after the generation of strong shock.

the upper atmospheres extend above photospheric layers in the later stage of simulation and the peak of density just below the photosphere becomes sharper

also in the later stage. The density gradient, which is the ratio of the difference of density between the maximum and the minimum below the photosphere to the difference of radii for the density maximum and minimum, is shown in Fig. 6. The gradient changes through the cycle but the mean gradient is

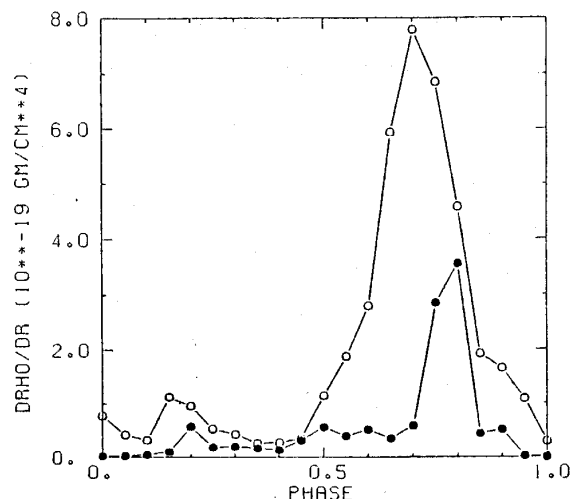


Fig. 6. Ratio of the density increase to the difference of radius. Abscissa is the phases of pulsation and ordinate is the ratio of the height of density-peak near the photosphere to the difference of radii for the maximum and the minimum of density. Filled circles indicate the cycle described in Fig. 5a and open circles express the cycle described in Fig. 5b.

remarkably great in the later stage. This suggests that the reflection surface of stellar oscillation would move to the layer just below the photosphere. This would be evidence for Takeuti's boundary conditions. We cannot decide what boundary conditions work in such large-amplitude pulsation, but the decrease of periods may be based on some hydrodynamical reason and we may note here, at least, Takeuti's conditions give a correct period for the present model.

We should also remark here that the apparent features of the variation of the luminosity and the photospheric radial velocity show only slight difference after the formation of extended atmospheres and the decrease of period. So we must pay much more attention to apply the period-mass-radius relation for low-surface gravity supergiant stars.

## §5. Conclusion

We have constructed a hydrodynamic model of less massive yellow supergiant stars. The recurrence of the generation of strong shock wave in the interval of several pulsation periods have been found as other authors obtained. We also obtained a sudden decrease of pulsation amplitude and period after the generation of strong shock. The amplitude grew up again but the decrease of period continued. We have also obtained that the peak of density distribution just



below the photosphere is sharpened after the formation of extended non-static atmospheres and the decrease of period seems to connect with this phenomenon. The outer boundary conditions for linear non-adiabatic pulsation described by Castor fail to derive the non-linear period. The other boundary conditions, which was proposed by Takeuti, give more suitable value in this case. We have the implication that the outer boundary conditions of radial pulsation still remain as an open problem.

This research was supported in part by the Grant-in-aid for Scientific Research of the Ministry of Education, Science and Culture under Grant No. 59540134. Computations were carried out at the Computer Center of Tôhoku University.

#### References

- 1) R.F. Christy: *Astrophys. J.* 145 (1966) 337.
- 2) D.A. Keeley: *Astrophys. J.* 161 (1970) 657.
- 3) V. Trimble: *Mon. Not. R. astr. Soc.* 156 (1972) 411.
- 4) P.R. Wood: *Mon. Not. R. astr. Soc.* 174 (1976) 531.
- 5) D.S. King: *Space Sci. Rev.* 27 (1980) 519.
- 6) Y. Tuchman, N. Sach and A. Barkat: *Astrophys. J.* 234 (1979) 217.
- 7) Yu.A. Fadeyev and A. Tutukov: *Mon. Not. R. astr. Soc.* 195 (1981) 811.
- 8) Yu.A. Fadeyev: *Astrophys. Space Sci.* 86 (1982) 143.
- 9) Yu.A. Fadeyev: *Astrophys. Space Sci.* 100 (1984) 329.
- 10) J.I. Castor, C.G. Davis and D.D. Davison: Los Alamos Scientific Laboratory Report, LA-6644 (1977).
- 11) T. Aikawa, K. Uji-iye, T. Okuda and M. Takeuti: *Science Reports Tôhoku Univ. Eighth Ser.* 3 (1982) 82.  
M. Takeuti, K. Uji-iye and T. Aikawa: *Science Reports Tôhoku Univ. Eighth Ser.* 4 (1983) 129.
- 12) T. Aikawa: private communication.
- 13) M. Takeuti: *Science Reports Tôhoku Univ. Eighth Ser.* 4 (1983) 126.
- 14) J.I. Castor: *Astrophys. J.* 166 (1971) 109.
- 15) M. Takeuti: *Publ. Astron. Soc. Japan* 16 (1964) 64.
- 16) N.H. Baker and R. Kippenhahn: *Astrophys. J.* 142 (1965) 868.